



A scheme for lunar inner core detection

James G. Williams¹

Received 20 September 2006; revised 5 December 2006; accepted 13 December 2006; published 9 February 2007.

[1] Very precise measurements of the lunar gravity field could detect a solid inner core. For synchronous rotation, the equator planes of the inner core and mantle should be tilted with respect to the ecliptic plane and precess along that plane with the same 18.6 yr period. Generally, two different tilts would cause a static inner core gravity field to appear as small periodic (27.212 d) variations in the mantle-referenced C_{21} and S_{21} coefficients. Tidal variations also contribute to the C_{21} variation so a much improved k_2 Love number would be required. Model computations suggest that the inner core signature is likely to be very small requiring sensitive gravity measurements. In principle, a signature analogous to the Moon's should be present for other synchronous satellites with interior liquid layers and also Mercury. **Citation:** Williams, J. G. (2007), A scheme for lunar inner core detection, *Geophys. Res. Lett.*, *34*, L03202, doi:10.1029/2006GL028185.

1. Introduction

[2] The free precession of the Earth's equator plane along the ecliptic plane is a familiar concept, but there is a fundamental difference for the precession of the Moon's equator. The precession of the Moon's equator is a forced precession. On the ecliptic plane, the descending node of the equator matches the ascending node of the orbit plane so that the orbit and equator planes precess together with the same retrograde 18.6 yr period. This arrangement, a Cassini state, depends on the synchronous rotation of the Moon. The amplitude associated with the lunar free precession damps by $1/e$ in 1.5×10^5 yr [Williams *et al.*, 2001] and has a small value [Newhall and Williams, 1997; Chapront and Chapront-Touze, 1997] while the forced precession amplitude does not damp.

[3] The Moon has a large solid mantle capped by the crust plus a small liquid core [Williams *et al.*, 2001]. A solid inner core has not been detected, but cooling of the fluid could lead to an inner core. It was predicted early [Goldreich, 1967] that the coupling between the mantle and fluid core would be insufficient to cause the fluid's orientation to closely follow the precessing mantle. The lunar laser results of Williams *et al.* [2001] confirmed weak coupling due to dissipation at the boundary. An oblate boundary can cause stronger coupling, but not enough to align the axes of rotation [Williams *et al.*, 2006b]. Still, there should be a small tilt to the fluid rotation with a precessing orientation.

[4] What would happen with an inner core? The coupling with the fluid is relatively weak allowing a different orientation. Any nonspherical attribute of the inner core gravity

field would result in torque on the inner core from the gravitational interaction with the Earth. In addition, there would be torque from gravitational interaction with the mantle. These gravitational torques should cause the mean inner core rotation period to match the mantle's, in the absence of strong nongravitational influences. It is shown in this paper that the inner core can have its own Cassini state, precessing with an 18.6 yr retrograde motion along the ecliptic plane. The tilt of the inner core's equator to the ecliptic plane can be different than the mantle's tilt. The distinct tilt and nonspherical gravity field of the inner core would cause a time variation of gravity measured on or above the lunar surface. The inner core can potentially be detected from this variation. The Moon can serve as a prototype for other solar system bodies with forced precession and an interior fluid layer.

2. Geometry

[5] The orientation of the mantle coordinate frame is known well from lunar laser range analysis [Williams *et al.*, 2006a] and serves as the reference frame for gravity field determinations [Konopliv *et al.*, 1998, 2001]. The mantle and inner core frames do not generally coincide and the potential of the inner core is referred to the mantle frame through a three angle rotation.

[6] Principal axis frames for the mantle and inner core allow their static second-degree gravity fields to be expressed in terms of J_2 and C_{22} . Here, the computations are simplified by assuming that (1) both mantle and inner core rotate with the same rate, (2) the two equator planes are tilted with respect to one another by a constant angle $I_m - I_{ic}$, and (3) small physical libration variations are ignorable. The mantle and inner core are treated as uniformly rotating and precessing with tilts I_m and I_{ic} , respectively.

[7] With small physical librations ignored, the angles from the descending nodes of the two equators to their principal-axis-defined zero meridians are $F + \pi + \tau_m$ for the mantle and $F + \pi + \tau_{ic}$ for the inner core. F is the orbit angle for the lunar mean argument of latitude with a period of 27.212 d and the τ s allow for a longitude shift between the principal axes of the zero meridians. When $\sin(I_m - I_{ic})$ is small, the inner core J_2 and C_{22} mostly transform into their corresponding constant mantle quantities, but there are small periodic effects. For unnormalized harmonic coefficients referred to the rotating mantle frame, using whole Moon mass (M) and radius (R), the most relevant of the periodic terms are

$$\Delta C_{21} = -\sin(I_m - I_{ic})\{J_2 \cos(I_m - I_{ic}) \sin(F + \tau_m) + C_{22}[1 + \cos(I_m - I_{ic})] \sin(F + 2\tau_{ic} - \tau_m)\} \quad (1a)$$

$$\Delta S_{21} = -\sin(I_m - I_{ic})\{J_2 \cos(I_m - I_{ic}) \cos(F + \tau_m) - C_{22}[1 + \cos(I_m - I_{ic})] \cos(F + 2\tau_{ic} - \tau_m)\}. \quad (1b)$$

¹Jet Propulsion Laboratory, California Institute of Technology, Pasadena, California, USA.

ΔC_{21} and ΔS_{21} are in the mantle frame while J_2 and C_{22} are in the inner core frame. For small $I_m - I_{ic}$, the ΔC_{21} variation is nearly proportional to the inner core $J_2 + 2C_{22}$ and the ΔS_{21} variation is nearly proportional to $J_2 - 2C_{22}$. There are other periodic terms among the five second-degree harmonic coefficients with arguments of $2F$, $3F$, and $4F$, but they involve second through fourth degree functions of $\sin(I_m - I_{ic})$, respectively.

3. Precession Dynamics

[8] The rotation dynamics considers three coupled units: the solid mantle including crust (subscript m), the fluid outer core (f), and the solid inner core (ic). For each unit, time-varying rotation about three axes depends on torque vectors. In addition to uniform rotation and precession, there will be oscillations about the uniform motion. These oscillations are about 0.03° for the mantle, compared to $I_m = 1.543^\circ$, and this paper concentrates on the tilts of the three precessing equators without oscillations.

[9] The two solid units are affected by torques from the Earth's gravitational attraction, \mathbf{T}_{me} and \mathbf{T}_{ice} . The orbit is taken to be circular. There are torques at the two fluid/solid interfaces due to oblate boundaries, \mathbf{T}_{fm} and \mathbf{T}_{fic} on the fluid, while the torques on the adjacent solid units will have opposite signs. The exterior gravity harmonics of the inner core can interact with the interior harmonics of the mantle with torques \mathbf{T}_{icm} on the inner core and $-\mathbf{T}_{icm}$ on the mantle. There are no gravitational torques on a uniform density fluid and therefore its rotation rate can differ from the solid units.

[10] The torques on the mantle, fluid, and inner core units are

$$\mathbf{T}_m = \mathbf{T}_{me} - \mathbf{T}_{fm} - \mathbf{T}_{icm} \quad (2a)$$

$$\mathbf{T}_f = \mathbf{T}_{fm} + \mathbf{T}_{fic} \quad (2b)$$

$$\mathbf{T}_{ic} = \mathbf{T}_{ice} - \mathbf{T}_{fic} + \mathbf{T}_{icm}, \quad (2c)$$

respectively. If high frequency terms and dissipation effects are ignored and the assumptions of the previous section are adopted, all of the precession causing torques will be aligned or anti-aligned at the common line of nodes. For each of the three units, the line-of-nodes component of the sum of torques can be set equal to the cross product of the precession rate vector and each angular momentum vector, giving three coupled differential equations.

[11] The three coupled differential equations are solved for the tilts of the equator planes to the ecliptic plane for the mantle (I_m), fluid core (I_f), and inner core (I_{ic}). The orbit plane inclination i is known. Each of the torques is proportional to a sine of angle combinations: $i + I_m$ for \mathbf{T}_{me} , $i + I_{ic}$ for \mathbf{T}_{ice} , $I_m - I_f$ for \mathbf{T}_{fm} , $I_{ic} - I_f$ for \mathbf{T}_{fic} , and $I_m - I_{ic}$ for \mathbf{T}_{icm} . The equations are linearized for sines of the four separate angles by setting the cosines equal to 1 as well as other suitable approximations. They are then inverted to get the sines of I_m , I_f , and I_{ic} . Tilt I_m is known to be 1.543° from lunar laser ranging data analysis, but it is treated as a solution parameter here with a well known coefficient in \mathbf{T}_{me} .

[12] Principal axis longitude shifts τ_m and τ_{ic} can result from the mantle's interior S_{22} harmonic and the size depends on both interior 2,2 harmonics. There is a balance

of the mean torques normal to the two equators. If the lunar mantle's interior S_{22} harmonic is comparable to its C_{22} harmonic, then $|\tau_{ic}|$ would be of order 20° while the relatively small core moment would make $|\tau_m|$ of order $20''$ which can be ignored here. The longitude shifts will be smaller if the symmetry axis of the mantle's interior 2,2 harmonics is more nearly aligned with its principal axis, which could happen if there is a common origin such as an ancient frozen figure due to equilibrium distortion from tide plus spin [Jeffreys, 1915, 1937; Kopal, 1969; Lambeck and Pullan, 1980].

4. Model Calculations

[13] For the dynamical computations of this paper, a lot is known about the mantle parameters, but little is known about the fluid outer and solid inner cores. The mantle (+ crust) has more than 98% of the lunar mass and there is little difference between the gravity coefficients of the mantle and the whole Moon. The whole Moon gravitational harmonics are known from spacecraft data analysis [Lemoine *et al.*, 1997; Konopliv *et al.*, 1998, 2001]. Lunar laser ranging data analysis gives accurate information on the orientation and rotation of the lunar mantle [Dickey *et al.*, 1994; Williams *et al.*, 2006a] and moment differences [Konopliv *et al.*, 1998], radius limits for the core/mantle boundary [Williams *et al.*, 2001], and early results on that boundary's oblateness [Williams *et al.*, 2006b]. By contrast, nothing is known about the real size of the inner core or the oblateness of the inner core/outer core boundary. There is no measurement of the mantle's gravity field interior to the core/mantle boundary or the inner core gravity field.

[14] For model calculations, a relatively large inner core is considered in order to emphasize the gravitational signature. The inner and outer core radii are fixed at 300 and 334 km, the two densities are suitable for solid and liquid iron (7800 and 7100 kg/m³, respectively), and the ratios of the two moments of inertia to the whole Moon moment come out 3.64×10^{-4} and 2.36×10^{-4} , respectively. The oblateness of the core/mantle boundary is fixed at 5×10^{-4} compatible with the fluid core radius [Williams *et al.*, 2006b]. In the first approximation, both the ΔC_{21} core signature and the inner core tilt I_{ic} depend on its $J_2 + 2C_{22}$. A spread of values was considered for $J_2 + 2C_{22}$ from 0 to somewhat larger than the whole Moon value, after scaling for the different masses and radii. Also, a spread of inner core/mantle coupling values was considered from absent to strong.

[15] Figure 1 shows three curves for inner core caused ΔC_{21} amplitude vs a spread of inner core $J_2 + 2C_{22}$ values. The inner core $J_2 + 2C_{22}$ values on Figure 1, expressed for the mass and radius of the inner core, were used for the tilt calculation; multiply by 3.58×10^{-4} to scale to the whole Moon MR^2 used in the Geometry section. The whole Moon $J_2 + 2C_{22}$ is 2.48×10^{-4} , so the inner core $J_2 + 2C_{22}$ values in Figure 1 range from 0 to 3×10^{-4} , the latter being 1.2 times the whole Moon value.

[16] A spread of mantle/inner core coupling strengths were computed. Three curves are presented in Figure 1. One case has no mantle/inner core coupling. The remaining cases were quantified according to the strength of the coefficient of $\sin(I_m - I_{ic})$ in torque \mathbf{T}_{icm} compared to the coefficient of $\sin(i + I_{ic})$ in \mathbf{T}_{ice} . For the second (moderate or

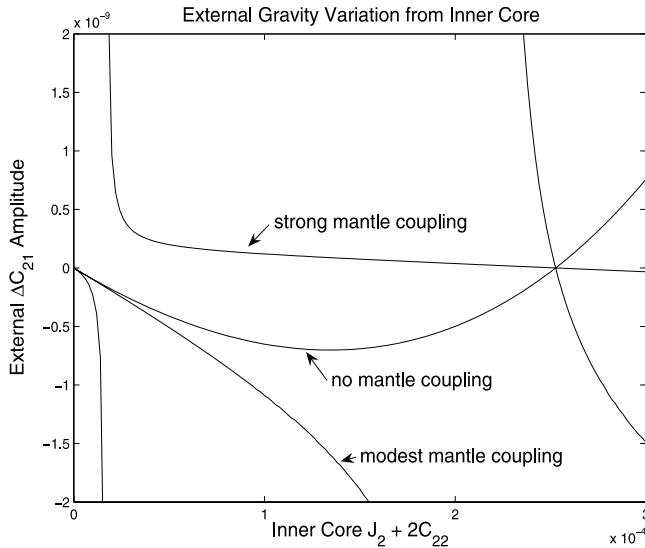


Figure 1. Amplitude of ΔC_{21} vs. inner core $J_2 + 2C_{22}$ for three inner core/mantle coupling strengths.

modest) case in Figure 1 this ratio was 4, while for the third (strong) case it was 64. For the inner core/mantle gravitational coupling parameter, an estimate of the topographic contribution to the mantle's internal J_2 can be made from early results on core/mantle boundary oblateness [Williams *et al.*, 2006b] and that favors the strong coupling case. For the ΔS_{21} amplitude, both inner core J_2 and C_{22} are needed. From the ratio of equation (1b) to (1a), $\Delta S_{21} = (J_2 - 2C_{22}) / (J_2 + 2C_{22}) \Delta C_{21}$ for small $I_m - I_{ic}$ so $\Delta S_{21} \leq \Delta C_{21}$.

[17] The sign of the ΔC_{21} coefficient reverses if $I_{ic} > I_m$ as equation (1) shows. This occurs near the whole Moon value of $J_2 + 2C_{22}$ in Figure 1, but the reversal location would shift if the inner boundary oblateness was finite. The precession dynamics has a resonance when the inner core's natural (free) precession period, an eigenvalue of the differential equations, matches the 18.6 yr retrograde forced precession. Such a resonance is apparent for the moderate and strong coupling cases in Figure 1 where the curves go off scale; it occurs for values beyond the right-hand frame boundary for the zero coupling case. To the left of the resonance value for the moderate and strong coupling cases, the tilt I_{ic} has a negative sign. For the strong coupling case, I_{ic} is within 0.1° of I_m for the right-hand half of Figure 1 and that accounts for the shallow curve there. The model computations for the inner core free precession period span several orders of magnitude. Analogous to the mantle [Ward, 1975], some model free precession periods now longer than 18.6 yr could have passed through resonance with the node as the Moon evolved outward. In Figure 1, the resonance shifts to the right as the orbit evolves outward and part of the area to the left of each curve's present resonance would have passed through the resonance. This would have been a major event for the core if it occurred.

5. Tides

[18] Solid-body tides also cause variations of the lunar gravity field and that must be considered when assessing the detectability of the inner core variation. The tidal components can be expressed as a series of periodic terms for

gravity harmonic coefficients. Table 1 shows the amplitudes for the two most important periods evaluated with a Love number k_2 of 0.0216, intermediate between two recent values [Williams *et al.*, 2006a, 2006b]. The 27.212 d pair of tidal terms has the same period as the inner core terms of interest, with $\sin F$ for C_{21} and $\cos F$ for S_{21} variations. Based on the foregoing model computations, a sensitivity of 10^{-10} or better is desired for the 2,1 harmonic coefficients, and that corresponds to 0.5% knowledge of the C_{21} tidal term. The current uncertainty for k_2 is about 12% [Konopliv *et al.*, 2001; Williams *et al.*, 2006a, 2006b] requiring considerable improvement. The 27.555 d (mean anomaly) tidal terms offer a possible way to improve the Love number while also trying to detect the inner core signature. For S_{21} , the inner core signature will be smaller than for C_{21} , but the tidal term is very much smaller with a current uncertainty of 1.2×10^{-11} .

6. Discussion

[19] Accurate orbital or surface measurements of periodic signatures in the gravity field of the Moon offer an opportunity to detect an inner core. Different tilts for precessing mantle and inner core equators would cause a static inner core gravity field to appear as a variable field in the mantle frame. The relatively small core makes the amplitudes of variation small. To detect the (mantle frame) ΔC_{21} amplitude of interest (equation (1a)), which is proportional to inner core $J_2 + 2C_{22}$, an order-of-magnitude accuracy improvement in the Love number k_2 is called for. This improvement might be achieved using the same gravity field measurements as the inner core search. The (mantle frame) ΔS_{21} variation is proportional to inner core $J_2 - 2C_{22}$ and should be the smaller of the 2,1 pair, but the tidal background is much less of a concern.

[20] Too little is known to reliably predict the strength of the inner core variations. A plausible spread of model parameter values is used for model computations and Figure 1 presents results for a spread of gravity coefficients and three inner core/mantle gravitational coupling strengths. A large (300 km radius) inner core was picked for the Figure 1 computations. The signal of interest is expected to scale as the fifth power of the inner core radius making detection harder for smaller cores. The scheme of this paper would require very high accuracy gravity field measurements, roughly 10^{-10} for a 300 km radius inner core and 10^{-11} for 190 km. Existing gravity fields based on past spacecraft missions do not achieve these accuracies. Very accurate future tracking data would be required to detect the inner core.

[21] The small lunar inner core effect stems from both cores relatively small sizes compared to the Moon. Several large synchronous satellites are suspected of having subter-

Table 1. Tidal Amplitudes (Unnormalized) for Two Major Tidal Periods

Gravity Coefficient	27.555 d Tide	27.212 d Tide
J_2	1.3×10^{-8}	0
C_{21}	0	-1.9×10^{-8}
S_{21}	0	-1.0×10^{-10}
C_{22}	7×10^{-9}	0
S_{22}	9×10^{-9}	0

reanean oceans, and for those cases the inner solid unit is large. Between the two solid units, relative motions in longitude, not equator orientation, was briefly mentioned by Wu *et al.* [2001]. An interesting extension of the scheme of this paper might be the possibility of detection of interior structure in large synchronous satellites with buried oceans. For satellites with equilibrium figures giving the same ratio C_{22}/J_2 for mantle and inner core, there is a plane intermediate between the mantle and inner core equators which nearly nulls the first-order signature analogous to equations (1), so a surface equator tilted with respect to the intermediate plane would indicate a fluid layer. Inner core-mantle coupling was considered for longitude librations for Mercury with its 3:2 rotation state [Peale *et al.*, 2002]; the obliquity is small and the equators of mantle and inner core are expected to nearly align which would minimize the gravity signature. Calculations for the satellites and Mercury would be necessary to see what is detectable.

[22] The detection of interior structure and properties is very difficult for the Moon and other remote bodies. The scheme of this paper, using high accuracy gravity field measurements, is offered as an additional technique.

[23] **Acknowledgments.** The development of the scheme of this paper was sparked by a question concerning accurate gravity data from A. Konopliv who also offered useful comments on the manuscript. The research described in this paper was carried out at the Jet Propulsion Laboratory of the California Institute of Technology, under a contract with the National Aeronautics and Space Administration.

References

- Chapront, J., and M. Chapront-Touzé (1997), Lunar motion: Theory, and observations, *Celestial Mech. Dyn. Astron.*, *66*, 31–38.
- Dickey, J. O., et al. (1994), Lunar laser ranging: A continuing legacy of the Apollo program, *Science*, *265*, 482–490.
- Goldreich, P. (1967), Precession of the Moon's core, *J. Geophys. Res.*, *72*, 3135–3137.
- Jeffreys, H. (1915), Certain hypotheses as to the internal structure of the Earth and Moon, *Mon. Not. R. Astron. Soc.*, *60*, 187–217.
- Jeffreys, H. (1937), On the figures of the Earth and Moon, *Mon. Not. R. Astron. Soc. Geophys. Suppl.*, *4*, 1–13.
- Konopliv, A. S., A. B. Binder, L. L. Hood, A. B. Kucinskis, W. L. Sjogren, and J. G. Williams (1998), Improved gravity field of the Moon from Lunar Prospector, *Science*, *281*, 1476–1480.
- Konopliv, A. S., S. W. Asmar, E. Carranza, W. L. Sjogren, and D. N. Yuan (2001), Recent gravity models as a result of the Lunar Prospector mission, *Icarus*, *150*, 1–18.
- Kopal, Z. (1969), *The Moon*, Springer, New York.
- Lambeck, K., and S. Pullan (1980), The lunar fossil bulge hypothesis revisited, *Phys. Earth Planet. Inter.*, *22*, 29–35.
- Lemoine, F. G. R., D. E. Smith, M. T. Zuber, G. A. Neumann, and D. D. Rowlands (1997), A 70th degree lunar gravity model (GLGM-2) from Clementine and other tracking data, *J. Geophys. Res.*, *102*, 16,339–16,359.
- Newhall, X. X., and J. G. Williams (1997), Estimation of the lunar physical librations, *Celestial Mech. Dyn. Astron.*, *66*, 21–30.
- Peale, S. J., R. J. Phillips, S. C. Solomon, D. E. Smith, and M. T. Zuber (2002), A procedure for determining the nature of Mercury's core, *Meteorit. Planet. Sci.*, *37*, 1269–1283.
- Ward, W. R. (1975), Past orientation of the lunar spin axis, *Science*, *189*, 377–379.
- Williams, J. G., D. H. Boggs, C. F. Yoder, J. T. Ratcliff, and J. O. Dickey (2001), Lunar rotational dissipation in solid body and molten core, *J. Geophys. Res.*, *106*, 27,933–27,968.
- Williams, J. G., S. G. Turyshev, D. H. Boggs, and J. T. Ratcliff (2006a), Lunar laser ranging science: Gravitational physics and lunar interior and geodesy, *Adv. Space Res.*, *37*(1), 67–71.
- Williams, J. G., D. H. Boggs, and J. T. Ratcliff (2006b), Lunar interior results and possibilities, *Lunar Planet. Sci.*, *XXXVII*, abstract 1229.
- Wu, X., Y. E. Bar-Sever, W. Folkner, J. Williams, and J. Zumberge (2001), Europa's tides and possible hidden liquid ocean—With new analyses on different orbit configurations and non-global ocean basins, *J. Geod. Soc. Jpn.*, *47*, 501–507.

J. G. Williams, Jet Propulsion Laboratory, California Institute of Technology, MS 238-600, 4800 Oak Grove Drive, Pasadena, CA 91109, USA. (james.g.williams@jpl.nasa.gov)